

OBSERVATIONS ON PREDICTION OF NON-SELF-SIMILAR SUBCRITICAL
CRACK GROWTH AND STRESS INTENSITY DISTRIBUTIONS

C. W. Smith

Department of Engineering Science and Mechanics
Virginia Polytechnic Institute and State University
Blacksburg, Virginia, 24061 USA

ABSTRACT

The present paper briefly describes a modified form of an experimental technique consisting of a marriage between the frozen stress photoelastic method and the local field equations of linear elastic fracture mechanics which can be used to estimate the stress intensity factor distribution in complex, three dimensional cracked body problems. The extension of the method to predict both flaw shapes and stress intensity distributions where neither are known a-priori along with accompanying limitations of the method are discussed. Use of the method is then illustrated by citing results obtained by applying it to three dimensional fracture problems from the aerospace and nuclear industries to show the differences which arise between results for real flaws and those assumed by analysts. It is concluded that, within prescribed limitations, the method exhibits good potential for providing computer code verification for numerical analyses in tracking sub-critical flaw growth and the accompanying stress intensity distributions in three dimensional cracked body problems.

KEYWORDS

Stress Intensity Factors, Surface Flaws, Three Dimensional Crack Problems, Photoelastic Analysis, Linear Elastic Fracture Mechanics, Experimental Stress Analysis, Sub-critical Flaw Growth, Real Cracks, Nozzle Corner Cracks.

INTRODUCTION

The majority of in-service fractures of structural components are preceded by the sub-critical growth of a flaw under cyclic loading until critical crack size is reached. The sub-critical or stable flaw growth stage usually involves complex geometric shapes, varying stress intensity factor levels along the flaw border, and non-planar flaws, resulting in a very difficult class of three dimensional (3D) cracked body problems which has resisted efforts of analysts to render them tractable in the full field sense. However, progress in numerical methods of analysis and improved digital computer storage capacities is resulting in more powerful approximate methods as noted by Rybicki and Benzley (1975). A major problem which remains is that of insuring proper formulation and tuning of complex, three dimensional numerical solutions for 3D cracked body problems through computer code verification in the form of an inexpensive proof test.

Nearly a decade ago, the writer and his colleagues, based upon an idea of Irwin (1958) began to evolve a technique consisting of a marriage between the field equations of linear elastic fracture mechanics (LEFM) and the frozen stress photoelastic method for estimating stress intensity factor (SIF) distributions in 3D cracked body problems. Originally proposed for Mode I loadings only by Smith (1975), the method was first modified by Jolles, McGowan and Smith (1975) and then extended by Smith (1980) to include mixed mode loads. After successful application to a number of technological problems such as those studied by Smith, Peters and Gou (1979) and Smith and colleagues (1979), it was noticed by Smith and Peters (1979) that natural crack shapes produced by the method were virtually identical to those produced by fatigue loads on steel structures by Broekhoven (1977).

The present paper briefly describes the modified method as currently being used and cites results of the use of the method in current 3D fracture problems in the aerospace and nuclear industries to show how real flaws differ from those often assumed by analysts. It is suggested that the method possesses potential for predicting both flaw shapes and SIF distributions for certain problems where neither are known a priori.

REVIEW OF ANALYTICAL CONSIDERATIONS (MODE I)

For the case of Mode I loading, one begins with equations of the form:

$$\sigma_{ij} = \frac{K_I}{r^{1/2}} f_{ij}(\theta) + \sigma_{ij}^0 \quad (1)$$

for the stresses in a plane mutually orthogonal to the flaw surface and the flaw border referred to a set of local rectangular cartesian coordinates as pictured in Fig. 1, where the terms containing K_I , the SIF, are identical to Irwin's Equations for the plane case and σ_{ij}^0 represent the contribution of the regular stresses to the stress field in the measurement zone. The σ_{ij}^0 are normally taken to be constant for a given point along the flaw border, but may vary from point to point. Observing that stress fringes tend to spread approximately normal to the flaw surface (Fig. 2), Eqs. 1 are evaluated along $\theta = \pi/2$ (Fig. 1) and

$$\tau_{\max} = 1/2 [(\sigma_{nn} - \sigma_{zz})^2 + 4\sigma_{nz}^2]^{1/2} \quad (2)$$

which, when truncated to the same order as Equations 1, leads to the two parameter Equation:

$$\tau_{\max} = \frac{A}{r^{1/2}} + B \quad \text{where} \quad \begin{aligned} A &= K_I / \sqrt{8\pi} \\ B &= f(\sigma_{ij}^0) \end{aligned} \quad (3)$$

which can be rearranged into the normalized form

$$\frac{K_{AP}}{q(\pi a)^{1/2}} = \frac{K_I}{q(\pi a)^{1/2}} + \frac{f(\sigma_{ij}^0)(8)^{1/2}}{q} \left(\frac{r}{a}\right)^{1/2} \quad (4)$$

where $K_{AP} = \tau_{\max}(8\pi r)^{1/2}$ and, from the Stress-Optic Law, $\tau_{\max} = Nf/2t'$ where N is the stress fringe order, f the material fringe value and t' the slice thickness in the t direction, q is the remote loading parameter (such

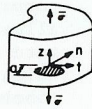


Fig. 1 General Problem Geometry and Notation for Mode I



Fig. 2 Typical Mode I Fringe Pattern

as uniform stress, pressure, etc.) and a the characteristic flaw depth. Equation (4) prescribes that, within the zone dominated by Equations (1) with σ_{ij}^0 as described above, a linear relation exists between the normalized apparent stress intensity factor and the square root of the normalized distance from the crack tip. Thus, one need only locate the linear zone in a set of photoelastic data and extrapolate across a very near field non-linear zone to the crack tip in order to obtain the SIF. An example of this approach using data from cracked plate tests described in the sequel is given in Fig. 3.

By following similar arguments, but not specifying $\theta = \pi/2$, equations for the Mixed Mode case have been developed by Smith, Jolles and Peters (1977).

EXPERIMENTAL PROCEDURE

The experimental procedure begins with the casting of parts of a scale model of the prototype structure out of suitable stress freezing photoelastic materials. Such materials possess diphasic properties which are similar to those of a Kelvin material. That is, at room temperature, the material exhibits time dependent behavior under load, while above critical temperature, in addition to being an order of magnitude more sensitive to load optically and two orders of magnitude less stiff, it responds in an essentially elastic, time independent manner to load except in the very near field non-linear zone ahead of a crack. Since the majority of cracks encountered in service originate at a specimen surface, only those will be discussed here. Starter cracks must be inserted into the cast part. If the crack is to represent a mechanically induced crack, it can be produced by striking a sharp tapered blade held normal to the specimen surface. The blade tip will indent the specimen surface slightly and a crack will emanate from the indented region forming a nearly semi-circular border which subsequently arrests. Thermal flaws with larger surface lengths than depths can be produced in the same way after a thermal gradient is produced across the specimen thickness.

Once the starter crack is produced, the cast parts of the scale model are assembled and glued together, taking care not to locate a crack or its path near a glue line. After assembly, the cracked model is placed in a temperature controlled stress freezing oven, heated to critical temperature and loaded sufficiently to grow the starter crack to its desired size. Upon reaching this size as viewed through a glass port in the oven, the load is reduced, terminating crack growth and the specimen is cooled under a reduced load to room temperature, freezing in the optical stress fringe system and deformation field produced above critical temperature. Due to the relative insensitivity of the material to load both optically and in mechanical deformation at room temperature, the model may then be unloaded with negligible optical or mechanical recovery. Moreover, slices may be removed from the model (normally mutually orthogonal to the flaw surface and the flaw border, i.e. parallel to nz plane, Fig. 1) without altering the "frozen in" stress fringe and deformation fields. These slices are then coated with a matching index fluid and analyzed in a crossed circular polariscope at about 10X using white light and employing the Tardy Method for obtaining fractional fringe orders. Results are

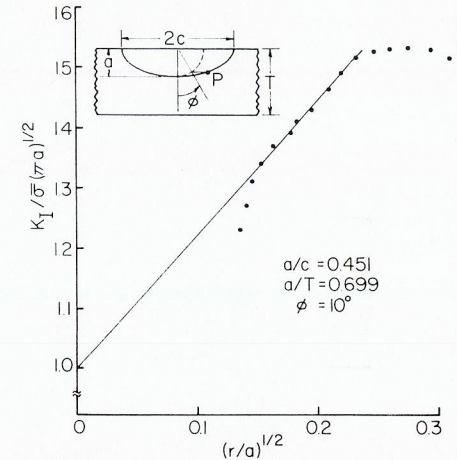


Fig. 3 Estimation of Normalized SIF from Frozen Slice Data

displayed as shown in Fig. 3 and the normalized stress intensity factor is estimated from such a graph for each slice location around the flaw border.

As shown by a survey of current test data in Fig. 4, a substantial variation in aspect ratio (a/c) can result in shallow flaws depending upon the starter crack aspect ratio. Moreover, for deep flaws ($a/T > 0.5$) the flaw shapes tend to deviate from semi-ellipses.

RESULTS FROM USE OF METHOD

In this section, we discuss the results of the application of the foregoing method to two current problems taken from the aerospace and nuclear industries, respectively.

Problem No. 1 - (Surface flaws in flat plates under remote uniform uniaxial tension.) A best estimate numerical solution has recently been provided by McGowan and colleagues (1980) for certain size semi-elliptic surface flaws. Analysts also often imply self-similar flaw growth in this problem. However, experiments such as those of Collipriest (1971), Sommer, Hodulak and Kordisch (1977) and Smith and colleagues (1980) reveal that, once the crack has penetrated to near mid-depth of the plate, the flaw shape begins to deviate from that of a semi-ellipse, producing a change in the accompanying SIF distribution. The assumed analytical crack size is pictured in Fig. 3 and Fig. 5 shows how a real flaw deviates from a semi-elliptic shape of the same aspect dimensions. Fig. 6 shows how the flaw shape deviation alters the experimental results from best estimates predicted by numerical analysis for semi-elliptic shapes. The experimental results are taken from the work of Smith and colleagues (1980) and the theoretical results and from McGowan and colleagues (1980). The experimental results here are believed to be lowered near $\phi = 90^\circ$ due to some unwanted out of plane bending but the SIF elevation near $\phi = 0$ is believed to be accurate.

Problem #2 - (Nozzle corner cracks in nuclear reactors.)

Analysts usually model these cracks as quarter circular or quarter elliptic and imply self-similar flaw growth. In the first phase of this study, photoelastic models of flat plates containing central nozzles with a single corner crack normal to the uniform uniaxial plate tension were used to grow cracks to different depths and SIF distributions were obtained by the frozen stress method by Smith and Peters (1978). The local geometry and notation for the problem is given in Fig. 7(a). Results of these tests were compared with results from tension-tension fatigue tests on A508 reactor steel models with cracks at the same location obtained by Broekhoven (1977). Flaw shape comparisons are shown in Fig. 7(b) and show that:

(i) Flaw shapes from the two test programs exhibit the same shapes and for cracks of the same relative size they virtually overlay each other.

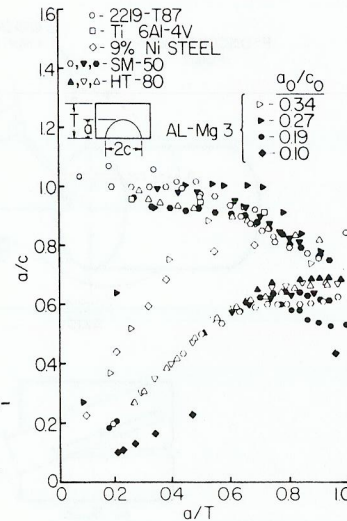


Fig. 4 Test Data from Literature for Uniaxial Tension
2219-T87 - Newman and Raju (1979)
Ti,6Al,4V - Hoepfner and Colleagues (1968)
Ni Steel - Nishioka and Colleagues (1977)
SM-50,HT-80 - Kobayashi and Colleagues (1977)
AL-Mg 3 - Sommer and Colleagues (1977)

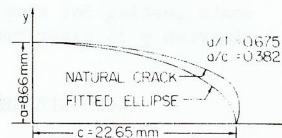


Fig. 5 Natural vs. Theoretical Crack Shape for Same Aspect Ratio

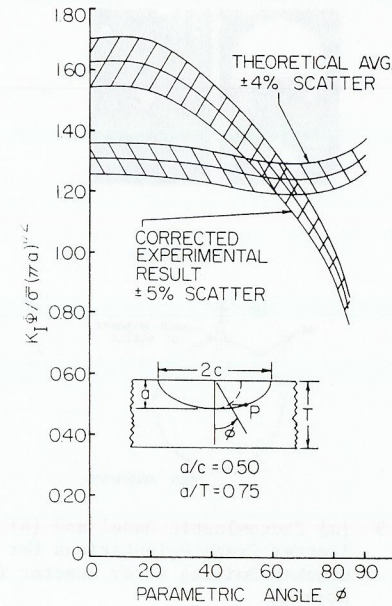


Fig. 6 Effect of Flaw Shape Deviations Upon SIF

(ii) Flaw shapes are not simple curves.

Broekhoven (1977) fitted a quarter ellipse to measured values of a_p and a_n and computed a SIF distribution using a finite element analysis. A comparison of such a computation with photoelastic results on the real flaw shape suggests that real cracks tend to take shapes which minimize the SIF gradient along the flaw border (Fig. 8).

Subsequent studies were conducted by Smith and colleagues (1979) on photoelastic models of boiling water reactor vessels containing cracks in nozzle corners. Each model contained two diametrically opposite cracked nozzles (Fig. 9a) with cracks in either the 0° or 45° orientations (Fig. 9b). For cracks in the 0° orientation, the tests confirmed the deviation of the cracks from quarter-ellipses (Fig. 10a) observed in the plate-nozzle tests and showed non-self-similar flaw growth accompanied by a continuously changing SIF distribution (Fig. 10b). Only one slice was analyzed for the smallest crack.

Cracks initiated from the 45° orientation remained in the initial flaw plane along the nozzle wall as they grew but underwent continuous reorientation of flaw plane near the vessel surface as they grew towards the plane normal to the vessel hoop stress direction (Fig. 11a). The shallow flaws acted as two different flaws joined at nv (Fig. 11a) but beyond $a/T \approx 0.3$, the discontinuous point (nv) on the crack front disappeared and a single non-planar crack resulted. Accompanying changes in the SIF distributions are shown in Fig. 11b.

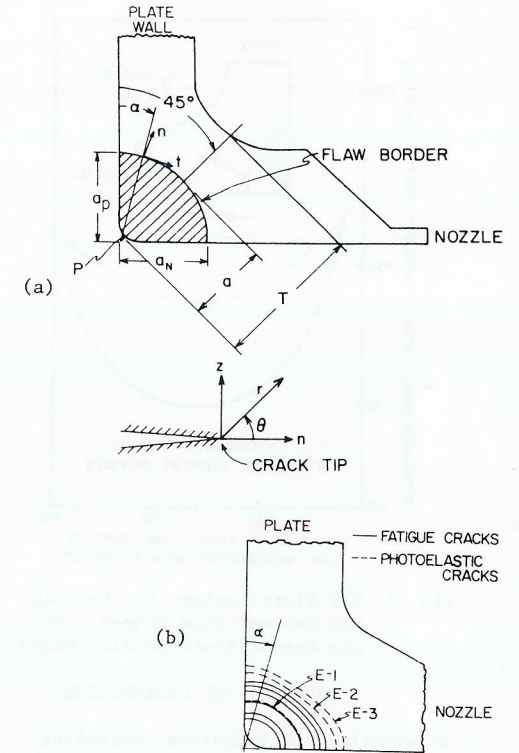


Fig. 7 (a) Problem Geometry, Notation and (b) Flaw Shapes for Nozzle Corner Cracks in Flat Plates

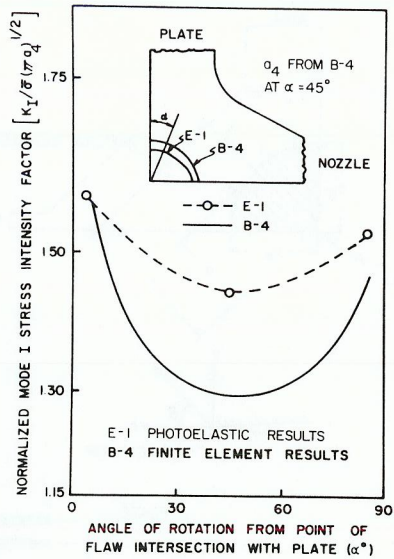


Fig. 8 SIF Distributions for Natural and Assumed Flaw Shapes - Nozzle Corner Crack in Flat Plate

SUMMARY AND OBSERVATIONS

An experimental technique consisting of a marriage between the frozen stress photoelastic method and the local field equations of linear elastic fracture mechanics was briefly reviewed. It's use as a computer code verification method was then illustrated by citing results from two kinds of problems where real cracks deviate from classical behavior assumed by analysts. It is observed that:

- (i) Sub-critical flaw growth generally produces complex flaw shapes and non-self-similar growth patterns.
- (ii) SIF distributions for real flaw shapes exhibit lower gradients along flaw borders than for assumed flaw shapes.
- (iii) SIF distributions change substantially with changes in flaw shape and orientations.

The method has its own limitations:

- (i) It is restricted to an elastic, incompressible material.

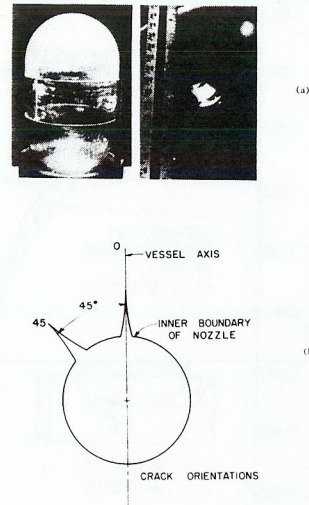


Fig. 9 (a) Photoelastic Model and (b) Starter Crack Orientations for Cracked Boiling Water Reactor (BW) Nozzles

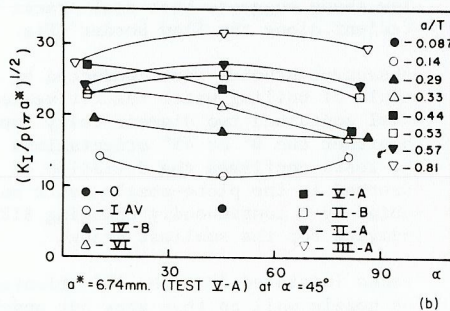
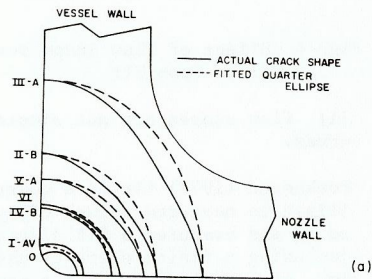


Fig. 10 (a) Flaw Shapes and (b) SIF Distributions for Cracked BWR Models at 0 Orientation

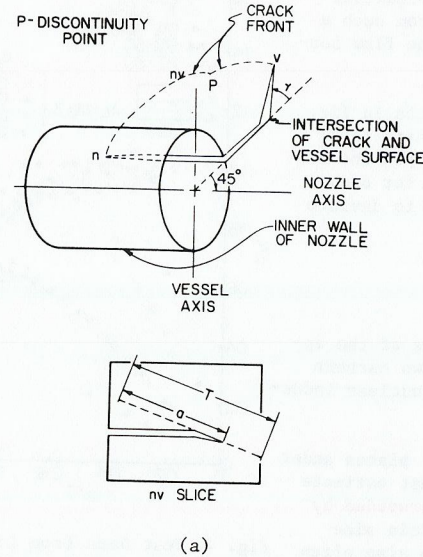


Fig. 11 (a) Flaw Geometry and (b) SIF Distributions for Cracked BWR Models at 45 degree Initial Orientation (beta is the angle in the plane of the initial flaw turned from the nozzle wall.)

- (ii) Initial flaw shape and size should be the same for model and prototype.
- (iii) Only small scale yielding should be permitted in the prototype.
- (iv) Fatigue loads should be tension-tension.

Nevertheless, the method is believed to offer a cost effective alternative to full scale testing for computer code verification of numerical analyses to within approximation +/- 5% experimental error for Mode I problems.

ACKNOWLEDGEMENTS

The writer gratefully acknowledges the assistance of the staff and facilities of the Department of Engineering Science and Mechanics of the Virginia Polytechnic Institute and State University, the encouragement of C. J. Astill and the support of the National Science Foundation under Grant No. Eng. 20824-1 for parts of his work.

REFERENCES

Broekhoven, J. J. G., (1977), "Fatigue and Fracture Behavior of Cracks at Nozzle Corners; Comparison of Theoretical Predictions with Experimental Data", Proceedings of Third International Conference on Pressure Vessel Technology, Part II, Materials and Fabrication, pp. 839-853.

Collipriest, J. E. (1971), "Part-Through-Crack Fracture Mechanics Testing", SD-71-319 Space Division, North American Rockwell.

Hoepfner, D. W.; Pettit, D. E; Fedderson, C. E. and Hyler, W. S. (1965), "Determination of Flaw Growth Characteristics of Ti-6Al-4V Sheet in the Solution Treated and Aged Condition", NASA CR-65811.

- Irwin, G. R. (1958), Discussion of the Paper "The Dynamic Stress Distribution Surrounding a Running Crack - A Photoelastic Analysis", Proc. of the Society for Experimental Stress Analysis, Vol. 16, No. 1, pp. 93-95.
- Jolles, M. I., McGowan, J. J. and Smith, C. W. (1975), "Use of a Hybrid, Computer Assisted Photoelastic Technique for Stress Intensity Factor Determination in Three Dimensional Problems", Computational Fracture Mechanics, ASME-SP, pp. 83-102.
- McGowan, J. J., Ed. (1980), "A Critical Evaluation of Numerical Solutions to the 'Benchmark' Surface Flaw Problem" (In Press), Experimental Mechanics.
- Newman, J. C. and Raju, I. S. (1979), "Analyses of Surface Cracks in Finite Plates Under Tension or Bending Loads", NASA TP/1578.
- Nishioka, K., Hirakawa, K. and Kitaura, I. (1977), "Fatigue Crack Propagation of Various Steels", The Sumitomo Search No. 17, pp. 39-55 (Available as ICAF-993).
- Rybicki, E. F. and Benzley, S. E., Eds. (1975), Computational Fracture Mechanics, ASME SP Computer Technology Committee of Pressure Vessels and Piping Division.
- Smith, C. W. (1975), "Use of Three Dimensional Photoelasticity and Progress in Related Areas", Experimental Techniques in Fracture Mechanics, 2, A. S. Kobayashi, Ed., pp. 3-58.
- Smith, C. W. (1980), "Photoelastic Determination of Stress Intensity Factors" (In Press), Mechanics of Fracture VI, G. C. Sih, Ed., Sitjhoff & Noordhoff International, Alphen aan den Rijn, The Netherlands.
- Smith, C. W., Peters, W. H. and Gou, S. F. (1979), "Influence of Flaw Geometry on Hole-Crack Stress Intensities", Fracture Mechanics, ASTM STP 677, pp. 431-445.
- Smith, C. W., Peters, W. H., Hardrath, W. T. and Fleischman, T. S. (1979), "Stress Intensity Distributions in Nozzle Corner Cracks of Complex Geometry", Paper No. G4/4, Transactions of the Fifth International Conference on Structural Mechanics in Reactor Technology, Vol. G.
- Smith, C. W. and Peters, W. H. (1979), "Prediction of Flaw Shapes and Stress Intensity Distributions in 3D Problems by the Frozen Stress Method", Preprints of the Sixth International Conference on Experimental Mechanics, pp. 861-864.
- Smith, C. W., Jolles, M. I. and Peters, W. H. (1977), "Stress Intensities for Cracks Emanating from Pin Loaded Holes", Flaw Growth and Fracture, ASTM STP 631, pp. 190-201.
- Smith, C. W., Peters, W. H., Kirby, G. C. and Andonian, A. (1980), "Stress Intensity Distributions for Natural Flaw Shapes Approximating 'Benchmark' Geometries", Thirteenth National Symposium on Fracture Mechanics.
- Sommer, E., Hodulak, L. and Kordisch, H. (1977), "Growth Characteristics of Part-Through Cracks in Thick-Walled Plates and Tubes", ASME Journal of Pressure Vessel Technology, Vol. 99, No. 1, pp. 106-111.